ISBN: 978-3-95450-197-7 doi:10.18429/JACoW-RUPAC2018-TUPSA29

EMITTANCE MEASUREMENT ON KRION-6T ION SOURCE BY PEPPER-POT METHOD

S. Barabin†, A. Kozlov, T. Kulevoy, D. Liakin, A. Lukashin, D. Selesnev, Institute for Theoretical and Experimental Physics of NRC Kurchatov Institute, Moscow, Russia
E. D. Donets, E. E. Donets, Joint Institute for Nuclear Research, Dubna, Moscow Region, Russia

Abstract

The Krion-6T ion source is an electron string ion source (ESIS) of multicharged ions. It will be used as an ion source for the heavy ion linac at the NICA project, but has been tested on an existing injection facility - Alvarez-type linac LU-20 with new RFQ type fore-injector. The transverse emittance measurements were carried out on the initial part of channel (IPC) of the low energy beam transport (LEBT) channel, between the ion source and RFQ fore-injector by pepper-pot method. Beams of multicharged Argon and Xenon ions are observed. Measurements of the profile and emittance were performed over several energies for each type of ions. The results of the measurement are presented, and some points of emittance calculations are considered.

INTRODUCTION

The Nuclotron-based Ion Collider fAcility (NICA) project at JINR (Dubna) has a goal to set up experimental studies of both hot and dense strongly interacting baryonic matter and spin physics. The experiments will be performed in collider mode and at fixed target [1]. The first part of the project program requires heavy ion collisions generation of $^{179}Au^{79+}$ nuclei. The beams at required parameters will be delivered by two superconducting synchrotrons: the Booster and the Nuclotron. The injector for the designed Booster ring is the new heavy ion linear accelerators HILAc (Heavy Ion Linear Accelerator) for the $^{179}Au^{31+}$beams with new ESIS type ion source Krion-6T [2] (for high charge state heavy ions). The source was optimized for production of ions with charge to mass ratio of $q/A \geq 1/3$ in order to provide complex test of all its systems at operation on existing injection facility. The source was installed at High-Voltage (HV) platform of the LU-20 fore-injector. Beam of Ar^{16+} was accelerated and extracted for users.

Low Energy Beam Transport Channel

The ion source is situated on high-voltage platform (up to 150 kV). The LEBT channel [3] (Fig. 1) begins from electrode with potential U0, after which a DN 250 vacuum valve is installed. In initial part of channel (IPC) the focusing electrodes with potentials U1 and U2 are located. IPC ends the tube with potential, falling off from U3 up to 0. Two solenoids, placed after initial part, form beam at the input of RFQ.

The emittance of the KRION-6T source was estimated in [4], and for a beam pulse duration of 8 μs, the 4 rms emittance value from the source should be 0.6 mm mrad. On the other hand, for $q/A \geq 1/3$ RFQ cavity require 1.5 π mm mrad input beam emittance [1]. To test KRION-LEBT-RFQ compatibility and check KRION-LEBT channel quality, emittances before the RFQ input should be measured.

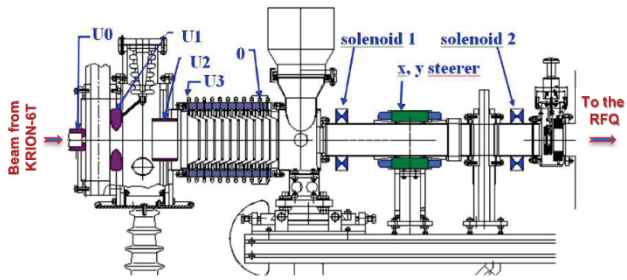

Figure 1: The LEBT Channel.

EXPERIMENTAL SETUP

The beam emittance before entering RFQ was measured at the IPC LEBT exit, since this is the only place where the emittance meter can be installed without moving both the KRION-6T source and RFQ cavity. To mounting the emittance meter, a final part of the LEBT channel was disassembled, and the emittance meter was installed after the IPC of LEBT (Fig. 2).

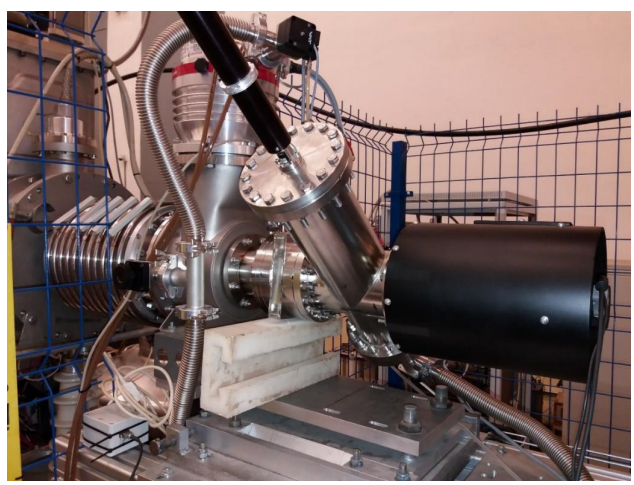

Figure 2: Emittance Meter.

† barabin@itep.ru

ISBN: 978-3-95450-197-7 doi:10.18429/JACoW-RUPAC2018-TUPSA29

An additional vacuum valve was installed between the IPC and the emittance meter to protect the source of the vacuum system from possible vacuum disasters in the emittance meter.

The emittance meter is a pepper-pot meter device [5]. Its main parts are a copper mask with a pattern of holes, and a scintillator behind it [5]. Both the mask and the scintillator are mounted together within a vacuum chamber on a rod of linear vacuum feedthrough. The copper mask receives an input ion beam from the source, and the holes in the mask break the beam on the set of beamlets, which hit the scintillator and produce a flash of light from it. The scintillation pattern consist mainly of a set of spots, and it is recorded by the VCD camera through a glass window on the opposite side of the vacuum chamber.

The VCD camera, which registers light from the scintillator, is mounted inside the external light shield on the beam axis, outside the vacuum chamber. The part of the emittance meter that registers the light has been specially redesigned to satisfy the limitations on the maximum length of the emittance meter. It was decided to mount an additional vacuum pump on a single free flange of the emittance meter vacuum chamber to satisfy strong vacuum requirements of the beam source. Because there was not enough space under the chamber to mounting the vacuum pump furniture on the flange, the emittance meter had to be rotated by 35° counterclockwise.

Common parameters of the emittance meter, the measurement procedure and the emittance calculation sequence are presented in [5]. Notable emittance meter parameters, specific for this series of measurements and not listed in [5], are: distance between a copper mask and a scintillator is 17 mm; distance from the beginning of the IPC to the mask plane is 1095 mm; VCD camera parameters: exposition is 3 ms, gain is 600.

MEASUREMENT MODES AND RESULTS

Emittances and profiles of ion beams from the Krion-6T source were measured. The measurements were carried out for 3 types of ions: Ar_{40}^{+16}, Xe_{124}^{+30}, Xe_{124}^{+41}. For each type of beam, two series of measurements were made. The 1-st series are measurements with different accelerating voltages on a high-voltage platform, from 20 to 75 kV with additional common extraction voltage about 3.6 kV, mainly series from 50 to 100 measurements for each mode. For accelerating voltages on a high-voltage platform of about 35 kV, a series of measurements with various beam currents was carried out.

Each beam contains several types of ions, for example, for Argon ions we have more than 80% of Ar_{40}^{+16} and less than 20% of Ar_{40}^{+15}; the same is true for Xenon beams. Each beam has an energy dispersion with a range of about 1.5 kV/nucleon. The measured beam charge at the IPC LEBT input is 2 nC, beam pulse duration is 8 μs, and beam current is 0.25 mA.

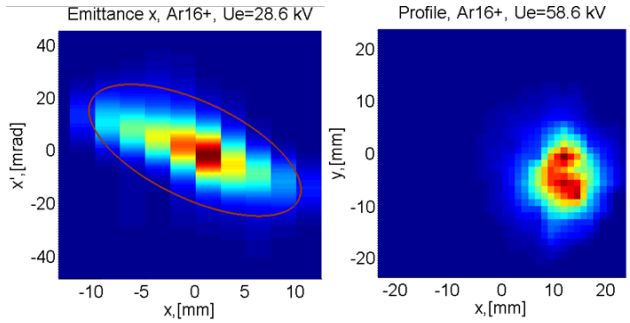

Figure 3: Beam phase space and profile examples.

The measurement processing program yields 2 main results: a beam image in the phase space along the x and y axes, and beam profiles (Fig.3). Based on that results, it is possible to calculate the main beam characteristics, such as: beam size and beam position, emittance and TWISS parameters values.

In most cases, the results are presented only for Argon beams; for Xenon beams, the results are the same, unless indicated otherwise.

Beam Profiles

An example of the beam profile for Argon ions is presented in Fig. 3, and the beam size from the accelerating voltage dependence for the Argon beam is shown on Fig. 4. It was observed that for each type of ions the beam size changed with the change in the accelerating voltage, and from Fig. 4 we see that an Argon beam, as well as the Xenon beams, has a well-defined crossover at a total (injecting + high voltage on platform) accelerating voltage of about 40 kV. In addition, it was found that the center of the beam was shifted from the center of the channel by 11.7 mm to the right and by 3.2 mm downwards for all beams.

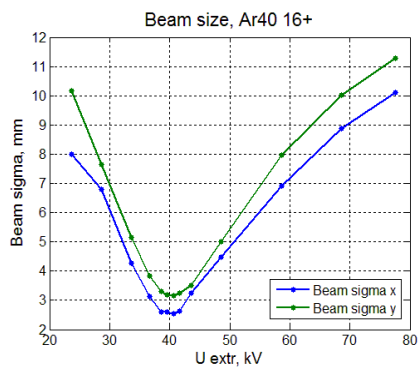

Figure 4: Beam size from accelerated voltages relations.

Compared beam sizes on a crossover for different beams, we see that the crossover voltages varies slightly for different types of ions: 40.5 kV for Ar_{40}^{+16}, 41.5 kV for Xe_{124}^{+41} and 43.5 kV for Xe_{124}^{+30}. That difference correspond with the mass/charge relations, which are 2.5, ~3 and ~4, in relative units, correspondingly. It should also be noted that the minimum beam size of different Xenon ion types is also different – for Xe_{124}^{+30} $\sigma_x = 2.53\ mm$, $\sigma_y = 3.15\ mm$, for Xe_{124}^{+41} $\sigma_x = 3.30\ mm$, $\sigma_y = 4.42\ mm$, i.e. beam size for higher charged ions is higher.

ISBN: 978-3-95450-197-7 doi:10.18429/JACoW-RUPAC2018-TUPSA29

Beam Emittances

Figure 5a shows the dependence of the normalized emittance of the argon beam on the accelerating voltage.

First, it should be noted that the calculated emittance values are only slightly larger than estimated previously [4] for a beam pulse duration of 8 μs, for most accelerating voltages. Secondly, the emittance values in the phase space y-y' are larger than the emittance values in the phase space x-x'. Thirdly, we observe a strange growth of emittance at higher accelerating voltages.

The cause of this emittance growth is the systematic error of the measuring device. As the accelerating voltage increases after the crossover, the transverse dimension of the beam on the scintillator also increases (see Fig. 4), hence the divergence angles of the ions should decrease, which leads to a decrease in the transverse dimensions of the spots from the beamlets. When the spots sizes are comparable to the size of the holes in the mask, it is necessary to take into account the non-zero size of the holes, recalculating the dimensions of the spots along the calibration curve [5]. In this case, a small change in the recorded spot size leads to a large change in its adjusted value. If the camera correctly registers the distribution of rays on the scintillator, this only leads to an increase in the measurement error (sometimes unacceptable). However, if the registered spot sizes are for any reason exceed the real, as the size of the spots decreased, the correction of the non-zero hole size becomes less and less reliable, which leads to an increase in the measured emittance value.

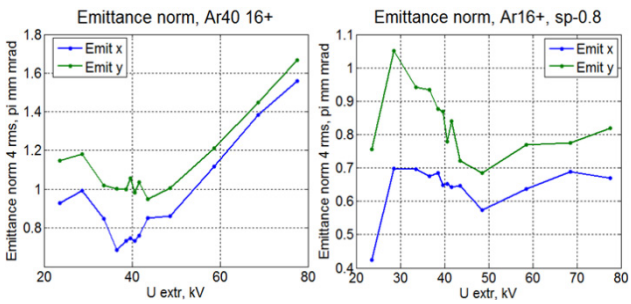

Figure 5: Normalized emittance from accelerating voltage relations, a) direct measurements, b) spot size correction.

Fig. 5b represent the results of an attempt to correct the spreading of spots. For this purpose, the size of all the spots were consistently reduced by a constant, until the emittance at high voltages did not cease to grow. On Fig. 5b the sizes of all the spots are reduced by 80 μm, which leads to compensation for the growth of the emittance.

The presented solution does not fully compensate emittance's growth due to the influence of background noise. Background noise can be compensated for at high light levels from a scintillator, but a decrease in the light level leads to an increase in detectable spot sizes from the beamlets and, consequently, to an increase in the emittance. This reason for the increase in the measured emittance value becomes dominant for small accelerating voltages, where a beam with a lower energy is distributed over a larger area; but this is also noticeable for high energies, where the increase in beam energy is compensated by its distribution over a larger area.

The presented realization of compensation for emittance growth is very rough, with an incorrect assumption for correction – the growth of the actual spot size will not be equal for all spots. It cannot be used to correctly determine the true emittance value, especially for large accelerating voltages. Despite this, this rough estimation allows you to check the reason why emittance is growing, and to estimate the growth of the emittance for more correct measurement conditions in the series. This increase in the emittance value for all types of ions is no more than 1.5 times.

CONCLUSION

Table 1 summarizes the measurement results.

Table 1: Results of Emittance Measurements

Measurement type	Ar_{40}^{+16}	Xe_{124}^{+30}	Xe_{124}^{+41}
Emit_x norm, 4rms, π mm mrad	0.86	0.66	0.86
Emit_y norm, 4rms, π mm mrad	1.00	0.80	1.09
Emit_x norm, spot compensated, estimated, 4rms, π mm mrad	0.57	0.44	0.54
Emit_y norm, spot compensated, estimated, 4rms, π mm mrad	0.68	0.55	0.77
Beam size on crossover, σ_x, mm	2.53	2.72	3.30
Beam size on crossover, σ_y, mm	3.15	3.35	4.42
x beam position, mm	11.63	11.76	11.68
y beam position, mm	3.12	3.37	3.16
Accelerated voltage on crossover, kV	40.5	43.5	41.5

The measured values of emittance after IPC LEBT correspond to the expected values, and these values are sufficient for subsequent acceleration in the RFQ cavity.

One of the main results of measurements was the detection of a crossover with accelerating voltages from 40 to 44 kV for different types of ions.

The most accurate emittance values can be obtained with an accelerating voltage of 48.6 kV. For another accelerating voltages a large measurement error is caused mainly by the blurring of the spots on the camera matrix, and also by background noise. The above measurements require additional clarification. This can be done using measurements with magnification several times the distance between the mask and the scintillator, mainly for high acceleration voltages.

ISBN: 978-3-95450-197-7 doi:10.18429/JACoW-RUPAC2018-TUPSA29

REFERENCES

[1] A. V. Butenko *et al*., "Development of the NICA Injection Facility", in *Proc IPAC'13,* Shanghai, China, May 2013, pp.3915-3917.

[2] E. E. Donets *et al*., "Status Report on Physics Research and Technology Developments of Electron String Ion Sources of Multicharged Ions", in *Proc. RUPAC'12*, Saint-Petersburg, Russia, Sep. 2012, pp. 208-212.

[3] A. V. Butenko *et al*., "The Heavy Ion Injector at the NICA Project", in *Proc. LINAC'14,* Geneva, Switzerland, Sep. 2014, pp. 1068-1070.

[4] A. V. Butenko *et al*., "Commissioning of the New Heavy Ion Linac HILac at the NICA Project", ", in *Proc. RUPAC'16*, Saint-Petersburg, Russia, Sep. 2016, pp.156-159, doi:10.18429/JACoW-RuPAC2016-FRCAMH03.

[5] S. Barabin *et al*., "Pepper-Pot Emittance Measurements", presented at RUPAC'18, Protvino, Russia, Oct. 2018, paper THPSC18, this conference.